

Physics of Planetary Systems — Exercises

Suggested Solutions to Set 1

Problem 1.1

(1 point)

Why are there so many different exoplanet detection methods in use?

Different methods are sensitive to different kinds of planets around different stars. As you can see in Fig. 1 different methods trace different regions in e.g. the $a - \mathcal{M}_{\text{pl}}$ -plane.

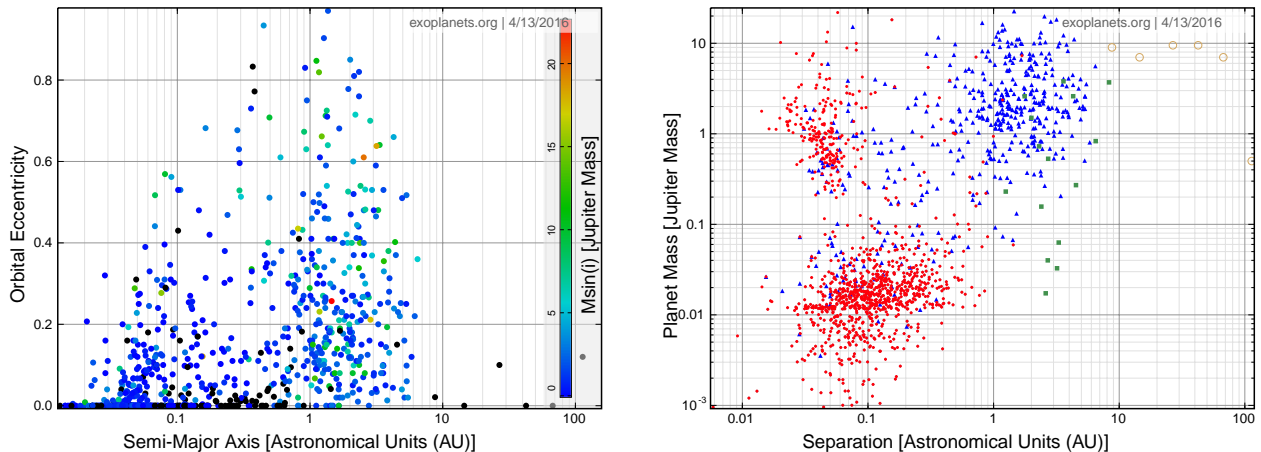


Figure 1: Distribution of a sample of known exoplanets in eccentricity, mass, and semi-major axis.

A few examples:

Transits:

- + Allows to find signal of low-massive planets
- + Very suited for high $R_{\text{pl}}/R_{\text{star}}$, very suited for M-dwarfs
- + Allows to probe the atmosphere of the planet
- geometric detection probability limits sample the further you move outwards
- you need a continuous coverage to not miss the transits
- Needs intelligent stacking of transits

Radial velocity:

- + Measures the dynamical parameters of the planet (mass, semi-major axis)
- Needs sufficient spectral lines, hence problems with hot stars
- Has to fight stellar variability

Microlensing:

- + Allows to find very distant planetary systems
- Many ambiguities in the derived parameters

Direct imaging:

- + Suited for massive & young planets in distant orbits
- + Allows for atmospheric characterization
- Advantage if host stars are less massive and fainter

Astrometry:

- + Sensitivity increases severely for stars close to our sun
- + Sensitivity increases severely for planets in wide orbits
- ...but also the observational baseline needed

Problem 1.2

(3 points)

(a) Orbital period, P , is related to semi-major axis, a , via Kepler's 3rd law:

$$P^2 \propto a^3 \quad \text{or} \quad P \propto a^{3/2}. \quad (1)$$

Hence we see a very clear correlation between a and P in Fig. 2.

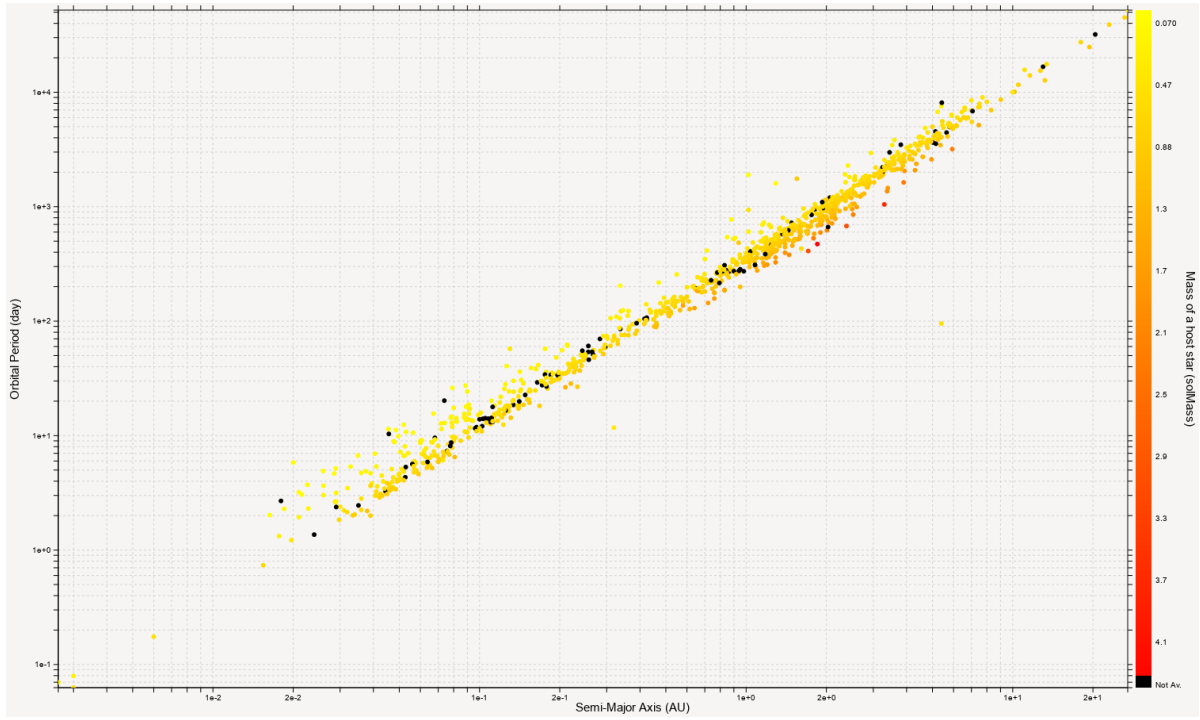


Figure 2: Distribution of a sample of known RV exoplanets over semi-major axis, orbital period, and host star mass.

(b) However, orbital period also depends on the masses of the orbiting bodies, in particular, the stellar mass:

$$P^2 = 2\pi \frac{a^3}{G(\mathcal{M}_* + \mathcal{M}_{\text{pl}})} \approx 2\pi \frac{a^3}{G\mathcal{M}_*}, \quad (2)$$

resulting in

$$P \propto a^{3/2} \mathcal{M}_*^{-1/2}. \quad (3)$$

The color-coded distribution of host star masses in Fig. 2 shows that, indeed stellar masses are the main cause for the observed scatter. Other effects (such as measurement errors and the contribution of the planet mass) are minor.

Bonus: Given that stars can have masses anywhere between $0.08 \mathcal{M}_\odot$ and $\approx 100 \mathcal{M}_\odot$, the observed scatter in P is surprisingly narrow, indicating that the host stars come in fact from a much narrower mass range. This reflects the fact stars similar to the Sun are favorable for some of the detection methods.

Problem 1.3

(1 point)

The estimate is trivial: if all $10^4 \dots 10^6 \mathcal{M}_\odot$ go into the stars, and the average mass of a star equals $1 \mathcal{M}_\odot$, we should get $10^4 \dots 10^6$ stars in $10^3 \dots 100^3$ pc, respectively, i.e., 1 star per cubic parsec. This is indeed comparable with the actual stellar density in the Milky Way disk. However, not all of the gas in the cloud goes into the stars (the so-called “star formation efficiency factor” is $\sim 20\%$), which would result in a lower stellar density. Besides, the newly-born stars have a distribution of masses (and the average stellar mass is actually below $1 \mathcal{M}_\odot$). This would have the opposite effect: the stellar density would be higher, and dominated by low-mass stars.